

# A semi-analytical model for velocity profile at wind turbine wake using blade element momentum

## Authors

Razieh Hamedi<sup>a</sup>  
Alireza Javaheri<sup>b</sup>  
Omid Dehghan<sup>c</sup>  
Farshad Torabi<sup>d\*</sup>

<sup>a</sup> Mechanical Engineering Faculty, K. N. Toosi University of Technology, Tehran, Iran

<sup>b</sup> Kiel University of Applied Science, Kiel, Germany

<sup>c</sup> Mechanical Engineering Faculty, University of Tehran, Tehran, Iran

<sup>d</sup> Mechanical Engineering Faculty, K. N. Toosi University of Technology, Tehran, Iran

## Article history:

Received : 8 December 2014

Accepted : 10 January 2015

**Keywords:** Semi-Analytical Model, Velocity Profile, Wind Turbine Wake, Blade Element Momentum.

## 1. Introduction

The problem of wind farm layout design concerns maximizing the energy gained from individual turbines in a special farm. The optimization is conducted over each individual turbine, considering the fact that the wake of a specific turbine affects wind velocity seen by the turbines that are located behind it. Consequently, to have a good estimation of the generated power of the turbines in the wake zone, one should be able to have a precise estimation of the wind velocity in the wake region.

## ABSTRACT

*The shape of wake behind a wind turbine is normally assumed to have a hat shape for the models used in wind farm layout optimization purposes; however, it is known from experimental tests and numerical simulations that this is not a real assumption. In reality, the results of actual measurements and detailed numerical simulation show that the velocity in wake region has a S-shape profile. The present study calculated a semi-analytical profile for the shape of the wake behind a wind turbine using blade element momentum method. It is shown that the wake shape differs in different operational conditions and geometrical characteristics of the wind turbine.*

A variety of models for wake velocity estimation has been proposed, which can be categorized into two main branches; namely numerical methods and theoretical methods, which try to give a simple equation for the decay of wake behind the turbine based on the fundamental governing equations. Numerical methods give more realistic and accurate results, though, they are very time consuming and are normally not suitable for optimization purposes. Theoretical methods, on the other hand, are efficient and accurate enough (if special considerations are taken into account) and very fast (because they give a simple explicit formula for the velocity deficit in the wake zone), which make them quite suitable for optimization purposes. In fact, at present,

\*Corresponding author: Farshad Torabi  
Address : Assistant Professor, Mechanical Engineering Faculty, K. N. Toosi University of Technology, Tehran, Iran  
E-mail address: ftorabi@kntu.ac.ir

most of the wind farm layout optimization problems are based on these types of models.

Jensen [1] proposed the very first model of wind wake behind a wind turbine, where he proposed a theory for wake distribution behind a wind turbine based on distance, wind speed, gaining induction, and entrainment constant from experiments using momentum theory. He used this theory in another article [2] to derive the total power of a wind farm. Mosetti [3] used the theory to optimize a wind farm by genetic algorithm optimization method. After that, many other researchers have tried to present different optimization algorithms using the proposed model of Jensen. Some of these articles [4-6] are concentrated on optimization algorithm and some others [7-9] on the function that is going to be optimized; i.e., the objective functions. There are few articles concerned about the wake model [10,11].

Frandsen [12] presented another wake model, which has more consistency with reality and in which the shape of the wake is a function of thrust coefficient which itself is a function of induction factor.

In all the above-mentioned articles, the shape of the wind behind a wind turbine was assumed to be a hat shape as was first proposed by Jensen [1]. In that article, Jensen himself noted that in reality, the shape of the wind behind a turbine was not a hat shape, but a bell shape. However, since it was not quite easy to calculate, a hat-shape profile was assumed by the author and the same profile was later used by all the researchers. In other words, in all the references mentioned above, the same wake shape was used for the wind profile in the wake zone.

The Jensen model and all the other inherited models have two distinct flaws. First, in all the models, the induction factor was assumed to be a specific constant, i.e.,  $a = 0.324$ , which was from the experimental measurements conducted by Højstrup [13]. This point was fully studied and discussed by Ghadirian et al. [14] and is not the scope of the present study. Secondly, even if we accept that the wake profile behind a wind turbine has a hat-shape profile, the value of the profile (the size of the hat) was not calculated correctly. In the original paper [1] Jensen assumed that the velocity just behind a wind turbine is  $v_0 = \frac{1}{3}u$  and later [2] he assumed that  $v_0 = 0.324u$ . Some researchers (for instance [3,4]) corrected this value to be  $v_0 = 2au$ . The assumption is not very

consistent with the theoretical and fundamental formulation of induction factor.

The present study aimed to (a) focus on the concept of the induction factor and explain its role in wake calculation, (b) use the concept of blade element momentum (BEM) theory to obtain the proper induction factor for different geometrical and operational conditions, and (c) calculate the hat-shape and bell-shape profiles behind a wind turbine.

## 2. Induction Factor

To understand the concept of the present work, a brief review of previous works is crucial. Figure 1 show the measured wake profile obtained from experimental tests [15]. As it can be seen, the actual measured data represents a bell-shape profile; however, Jensen [1] for simplicity assumed that the profile can be regarded as a hat-shape profile shown in the figure. Figure 2 shows the wind profile in the wake zone that was first proposed by Jensen [1] and is known as Jensen's model. In this model, the zone right after the turbine blades has not been considered because blades rotation in this zone and consequently rotation of the wind behind it causes a special kind of wake. In a reasonable distance behind the turbine, the wind profile takes a hat shape as shown in the figure. Considering the hat shape just after the wind turbine, and assuming a linear wake propagation, the continuity or conservation of mass results:

$$\pi r_0^2 v_0 + \pi(r_1^2 - r_0^2)u = \pi r_1^2 v \quad (1)$$

while  $u$  is wind speed at infinity,  $v_0$  is the wind speed right behind turbine and  $v$  is the wind speed at distance  $x$  after the turbine.  $r_0$  is the turbine radius and  $r_1$  is the wake radius at distance  $x$  after the turbine.

In this model, wake distribution behind the turbine has been assumed to be linear (Fig. 2). In addition, the velocity right after the wind turbine has been assumed to be  $\frac{1}{3}u$  based on previous theories. Therefore the velocity in the wake region is obtained from:

$$v = u \left( 1 - \frac{2}{3} \left( \frac{r_0}{r_0 + \alpha x} \right)^2 \right) \quad (2)$$

where  $\alpha$  is the wake distribution constant and has always been assumed to be around 0.1. This has been speculated and approved by Jensen [1] comparing the results with the data presented by Højstrup [13] for specific conditions.

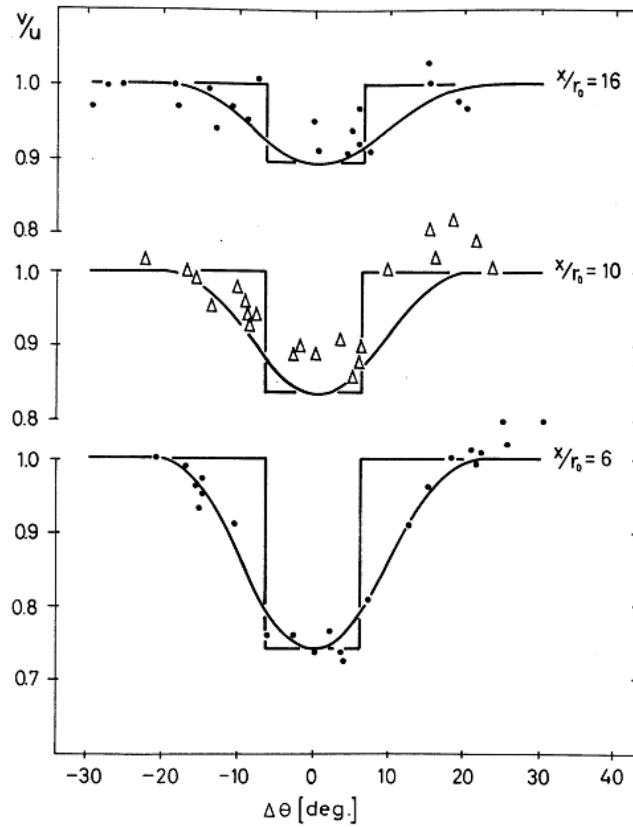


Fig.1. Experimental measured wind profile at turbine wake [15]

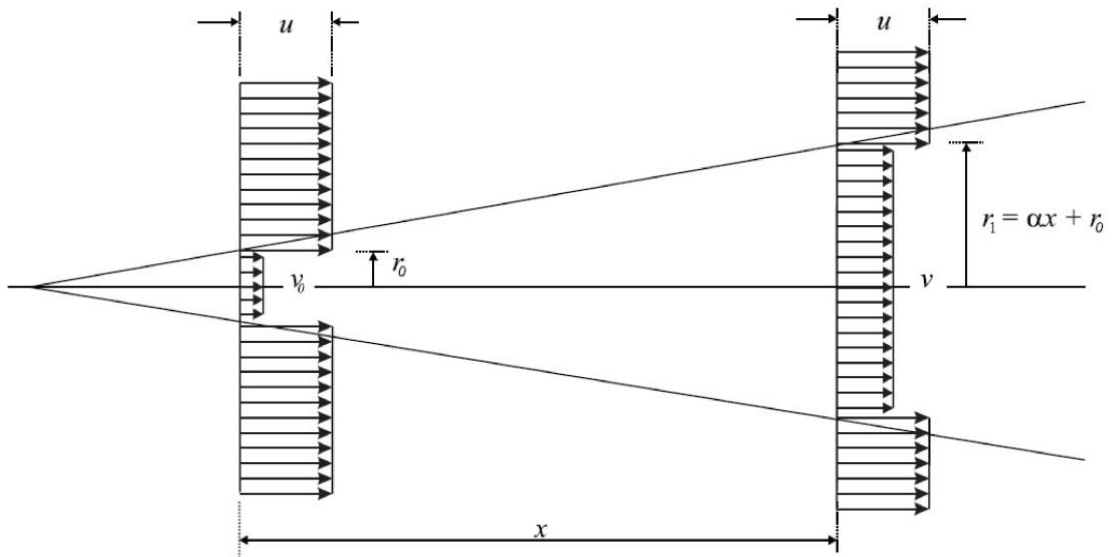


Fig.2. Schematic wake model of Jensen [1]

Mosetti [3] provided the following formula for deriving wake distribution constant:

$$\alpha = \frac{0.5}{\ln\left(\frac{z}{z_0}\right)} \quad (3)$$

where  $z$  is the hub height and  $z_0$  is the terrain surface roughness.

The important parameter in Eq. 2, which is

the concern of the present study, is the  $\frac{2}{3}$  coefficient that was obtained from the assumption of  $v_0 = \frac{1}{3}u$ . Jensen [1] defined induction factor as the ratio of the velocity just behind the wind turbine over the undisturbed wind velocity:

$$a = \frac{v_0}{u} \quad (4)$$

Hence, the induction factor was first assumed to be  $a = 1/3$  by Jensen [1] due to the similarity with Betz theory and reaching maximum  $C_P$  based on the one-dimensional momentum theory. Later on, Jensen [1] corrected this value to  $a = 0.324$  to reach more consistency with real site data conducted by Vermeulen [15] and Høistrup [13]. These data were gathered from a Nibe-A turbine with 20 meters diameter and in  $8.1 \text{ ms}^{-1}$  wind velocity in 100 meters hub height. Some other researchers (for example [3,4]) assumed:

$$\frac{v_0}{u} = 2a \quad (5)$$

that is not consistent with its definition. The main reason for this ambiguity is that, the induction factor is not a constant value as was assumed by nearly all the researchers. The value of induction factor is a function of different parameters including geometrical parameters such as blade profile, length and shape, and operational conditions such as wind velocity and rotational speed. Ghadirian et al. [14] considered these effects and gave a practical approach for calculating induction factor in different conditions. The importance of correctly calculated induction factor and its effect on wind farm optimization was fully discussed in that article and is not repeated here.

Before proceeding, the induction factor should be explained in more detail. When wind flows over a wind turbine, the rotational speed of blades, the skin friction, lift of the blades, and other aerodynamic parameters result into an induced rotational flow behind the turbine. The induced velocity can be projected into three orthogonal directions, namely, axial direction that is opposite to the wind direction, rotational direction that is in the same direction with the rotational speed, and blade wise direction that is usually very small and can be neglected. Neglecting the blade wise-induced velocity (which is one of the main assumptions in BEM method), the induced velocity is projected only in axial and rotational direction. The rotational velocity (Fig. 3) does not contribute to axial continuity or momentum balance, while the axial part plays an important role in wake calculations. Since the axial part of induced velocity is in the opposite direction of wind flow, it reduces the velocity seen by the turbine. In other words, if the undisturbed velocity is  $u$ , the velocity passes over the turbine blades is:

$$v_0 = u(1 - a) \quad (6)$$

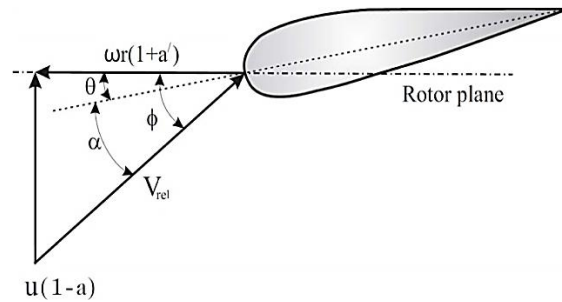


Fig.3. Schematic wake model of Jensen [1]

Now, if we take the whole wind turbine as a control volume, the continuity suggests that the velocity just behind the wind turbine becomes the same as one presented by Eq. (6). Incorporating Eq.6 into Eq.1, the actual velocity becomes:

$$v = u \left( 1 - (1 - (1 - a)) \left( \frac{r_0}{r_0 + ax} \right)^2 \right) \quad (7)$$

Equation 7 is the basic and fundamental equation that describes the wind velocity behind a wind turbine under a specific operational condition. Thus, to have an accurate result, the induction factor,  $a$ , should be calculated correctly instead of using a different formulation. If the proper induction factor is calculated, a hat-shape wind profile will be obtained by Eq.7. However, it is clear that the wake profile behind a wind turbine has a bell shape instead of hat shape. The rest of the article concerns about calculating a bell-shape profile for wind turbine.

### 3. Calculation of Bell-Shape Profile in the Wake Zone

#### 3.1. Velocity Profile Obtained from BEM Method

Ghadirian et al. [14] showed that the total induction factor for a wind turbine can be obtained using BEM method. In BEM method, the blade is divided into some segments (Fig. 4). Then, it is assumed that each segment does not interact with the other segments. By this assumption, the induction factor is obtained for each individual segment [14,16]; therefore, as can be seen in the figure, the mass flow rate can be obtained for each segment.

The above mentioned procedure shows that by means of BEM method, the wake profile behind the blade can be obtained as is illustrated in Fig.5. However, as it can be seen in this figure, the nacelle clearly has its own induction factor. Since the nacelle shape affects the wake shape, its geometry should

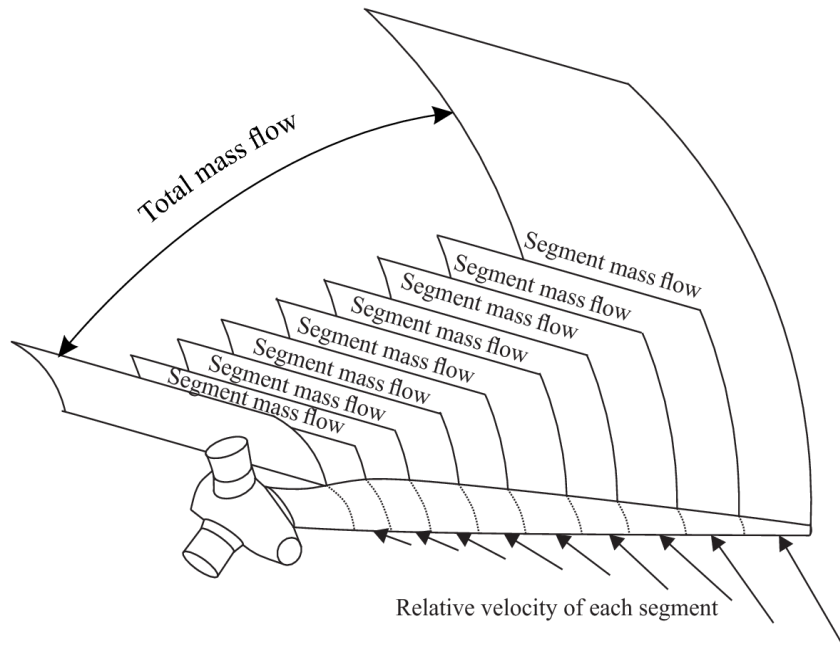


Fig.4. BEM concept

be analyzed numerically. But to obtain an analytical formulation, we can assume that the wake behind the nacelle has a third rate profile shape; that means:

$$v_{nacelle}(r) = a_1 r^3 + a_2 r^2 + a_3 r + a_4 r = 0..r_{root} r \quad (8)$$

where  $r_{root}$  is the radius of the first blade segment (used for BEM calculations).

The symmetry condition implies that  $a_3 = 0$ ; hence the other coefficients should be obtained. These values can be found by assuming that the flow is continuous behind

the turbine; this implies that the velocity at the blade root or the first segment of the blade (in BEM algorithm) should be equal to the velocity obtained from BEM method; in other words:

$$v_{nacelle}(r_{root}) = a_1 r_{root}^3 + a_2 r_{root}^2 + a_4 = u(1 - a_{root}) \quad (9)$$

where  $a_{root}$  is the induction factor at the first blade segment.

Second equation is obtained using the conservation of momentum. Considering the

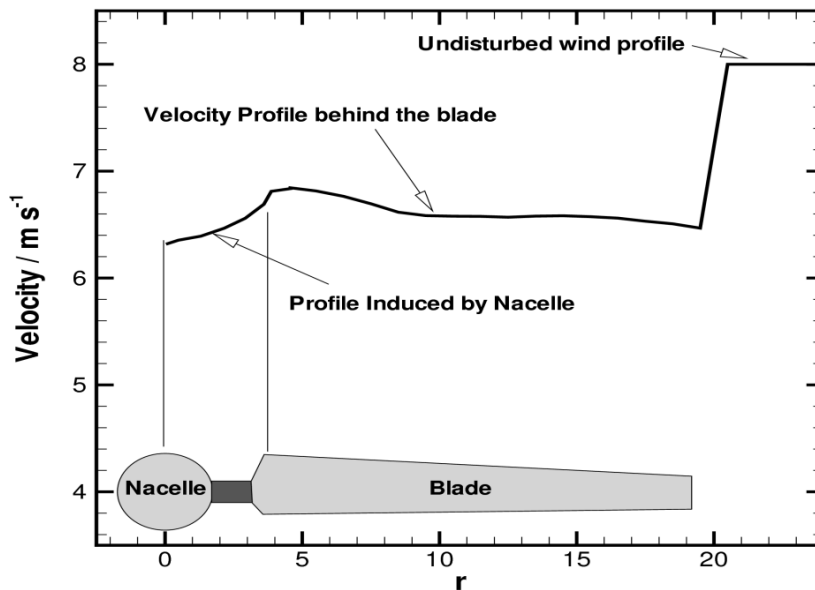


Fig.5.BEM concept

nacelle to have a blunt shape as shown in Fig.6, and writing a momentum balance, the total exerted force on the nacelle can be obtained as:

$$F = F_2 - F_1 \quad (10)$$

where  $F_1$  is the inlet momentum:

$$F_1 = \int \rho u^2 dA_1 = \rho u^2 A_1 \quad (11)$$

and  $A_1$  is the inlet area of nacelle control volume that is unknown and  $u$  is undisturbed velocity. Also  $F_2$  is the outlet momentum:

$$F_2 = \int \rho v_{nacelle}^2 dA_2 \\ = \int_0^{r_{root}} \rho (a_1 r^3 + a_2 r^2 + a_4)^2 (2\pi r) dr \quad (12)$$

By means of Eq.10, one can calculate the total exerted force on the nacelle,  $F$ . On the other hand the total exerted force on the nacelle can be obtained from:

$$F = \frac{1}{2} \rho C_D A u^2 \quad (13)$$

where  $C_D$  is the drag coefficient for the axis-symmetric blunt body.

The third-order polynomial profile should also satisfy the continuity equation or:

$$\rho u A_1 = \int \rho v_{nacelle} dA_2 \\ = \int_0^{r_{root}} \rho (a_1 r^3 + a_2 r^2 + a_4) (2\pi r) dr \quad (14)$$

Another equation is obtained by assuming zero curvature condition at the blade root:

$$r = r_{root} \rightarrow \frac{d^2(v_{nacelle})}{dr^2} = 0 \quad (15)$$

Equations 9 to 15 are used to obtain the wind profile induced by the nacelle.

### 3.2. Calculation of Total Axial Induction Factor

As mentioned before, BEM method calculates induction factor along the blade of wind turbine. But, a total induction factor is required to obtain the wind speed profile behind wind turbine. Ghadirian et al. [14] used axial induction factor of different radial distances of rotor calculated based on BEM theory, to derive the total induction factor as is described below.

As the total rate of mass flow crosses wind turbine rotor area equals to summation of those cross the area of each single segment (Fig.4), thus:

$$\dot{m}_{total} = \sum_{i=1}^{N_s} \dot{m}_{seg} \quad (16)$$

where  $\dot{m}_{total}$  is the total rate of mass flow crosses rotor area,  $\dot{m}_{seg}$  is rate of mass flow crosses each single segment area, and  $N_s$  is the number of segments.  $\dot{m}_{seg}$  is calculated as below:

$$\dot{m}_{seg} = \rho (1 - a_{loc}) u \pi (r_e^2 - r_s^2) \quad (17)$$

where  $r_e$  and  $r_s$  are outer and inner radius of each segment respectively, as shown in Fig.7.  $a_{loc}$  is the axial induction factor obtained through BEM theory.  $\dot{m}_{total}$  is calculated by

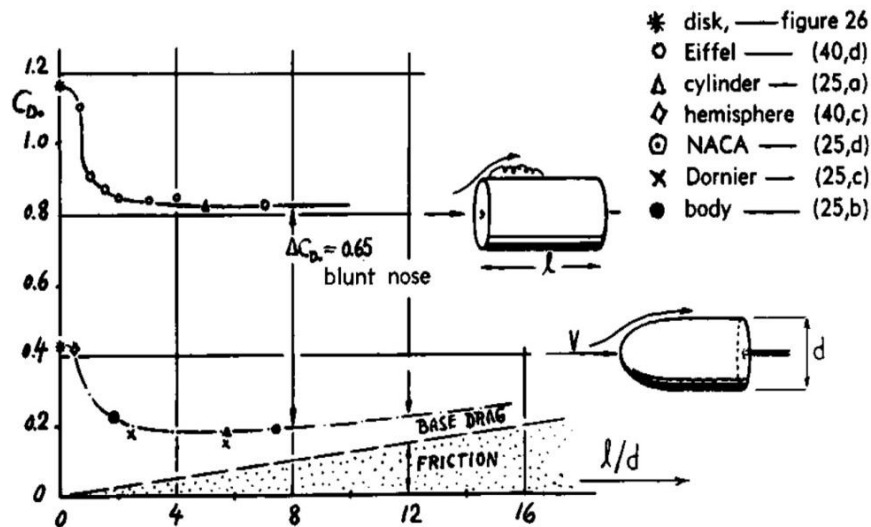


Fig.6. Drag of a blunt cylinder [17]

means of the following equation:

$$\dot{m}_{total} = \rho A_{total} v_0 \quad (18)$$

in which  $A_{total}$  is the total wind turbine rotor region. If one considers an assumed total induction factor, the velocity of flow in rotor area is:

$$v_0 = (1 - a_{total})u \quad (19)$$

then according to Eqs.16 to 19:

$$(r_{tip}^2 - r_{root}^2)(1 - a_{total})u = \sum_1^{N_s} (r_e^2 - r_s^2)(1 - a_{loc})u \quad (20)$$

total axial induction factor can now be calculated using Eq. 20:

$$a_{total} = 1 - \frac{\sum_1^{N_s} (r_e^2 - r_s^2)(1 - a_{loc})}{r_{tip}^2 - r_{root}^2} \quad (21)$$

where  $r_{tip}$  and  $r_{root}$  are the radius of tip and root of blade, respectively, as is observed in Fig.7.  $a_{loc}$  and  $a_{total}$  are local induction factor in an arbitrary radial distance and the total induction factor, respectively.

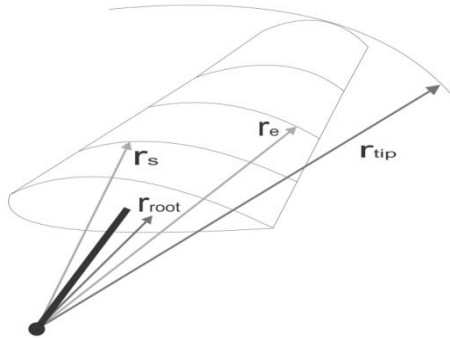


Fig.7.Radial distances of wind turbine blade

### 3.3. Calculation of Correlation between Decrease Rate of Velocity Deficit in the Center of Wake Behind Wind Turbine and Growth Rate of Wake Radius in Terms of Distance

In [18] general pattern of wake radius growth behind wind turbine, and decrease rate of velocity deficit in the center of wake behind wind turbine for far region is estimated as  $r_1 x^{\frac{1}{3}}$  and  $U_s x^{\frac{-2}{3}}$  where  $r_1$  is wake radius and  $U_s$  is velocity deficit in center of wake which is defined as:

$$U_s = u - U_c \quad (22)$$

Boundary conditions are necessary to obtain the correlation between decrease rate of velocity deficit in the center of wake behind wind turbine and growth rate of wake radius. In [19], the region from wind turbine

to the distance of twice as big as wind turbine diameter is considered close region and from this distance to infinity is considered far region. This method deals with Bernoulli equation for close region and derives wake radius and velocity deficit in the center line of wake in this region. Then they will be used as boundary conditions to find correlation between wake growth rate and velocity deficit decrease rate in the wake center downstream of wind turbine for far region. These equations are stated in the following.

According to Fig.8, applying Bernoulli equation between sections 1 and 2 leads to:

$$P_{in} + \frac{1}{2}\rho u^2 = P + \frac{1}{2}\rho v_0^2 \quad (23)$$

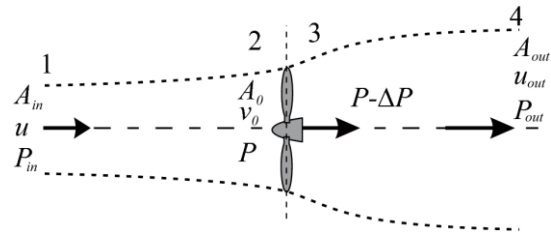


Fig.8.Sections in close region of wind turbine

Air experiences a pressure drop when it flows through wind turbine rotor. Bernoulli equation between sections 3 and 4 gives:

$$P - \Delta P + \frac{1}{2}\rho v_0^2 = P_{out} + \frac{1}{2}\rho u_{out}^2 \quad (24)$$

As previously cited, pressure in the inlet is assumed to be the same as that in outlet:

$$P_{in} = P_{out} \quad (25)$$

Combining Eqs. 23 and 24 results in:

$$\Delta P = \frac{1}{2}\rho(u^2 - u_{out}^2) \quad (26)$$

From momentum equation between sections 1 and 4, the pressure drop induced by wind turbine is obtained:

$$\Delta P = \rho v_0(u - u_{out}) \quad (27)$$

Equating Eqs. 26 and 27,  $v_0$  is calculated:

$$v_0 = \frac{1}{2}(u + u_{out}) \quad (28)$$

On the other hand, using induction factor definition:

$$v_0 = (1 - a)u \quad (29)$$

Equating Eqs. 28 and 29 gives rise to:

$$u_{out} = (1 - 2a)u \quad (30)$$

Applying continuity equation between

sections 2 and 4, wake diameter at the end of close region can be calculated:

$$D_{out} = D_0 \sqrt{\frac{1-a}{1-2a}} \quad (31)$$

where  $a, D_0, D_{out}$  are axial induction factor, rotor diameter and wake diameter in distance twice as big as rotor diameter, in other words, end of close region, respectively.

Impose of these boundary conditions in equations of decrease rate of velocity deficit in the center of wake behind wind turbine and growth rate of wake radius, enables one to find the following equations:

$$r_1 = r_{out} \left(\frac{x}{4r_0}\right)^{\frac{1}{3}} \quad (32)$$

and

$$U_s = 2au \left(\frac{x}{4r_0}\right)^{\frac{-2}{3}} \quad (33)$$

in the equations above, a specific axial induction factor must be used; here, the total axial induction factor obtained in section 3.2,  $a_{total}$  is considered instead of a constant axial induction factor suggested by Jensen. Thus:

$$U_s = 2a_{total}u \left(\frac{x}{4r_0}\right)^{\frac{-2}{3}} \quad (34)$$

In the same manner, Eq.31 can be written as:

$$D_{out} = D_0 \sqrt{\frac{1-a_{total}}{1-2a_{total}}} \quad (35)$$

#### 4. Analytic Calculation of Velocity Profile Just Behind Wind Turbine

In [18], general shape of velocity profile was estimated as an exponential function:

$$\frac{u-U}{U_s} = \exp(B\eta^2) \quad (36)$$

in which  $U_s$  is velocity deficit in wake center:

$$U_s = u - U_c \quad (37)$$

where  $U_c$  is velocity in wake center. The dimensionless radial distance,  $\eta$ , is determined by:

$$\eta = \frac{r}{r_1} \quad (38)$$

where  $r$  is an arbitrary radial distance. Since Eq.36 cannot predict the wind speed profile with an appropriate agreement with

experimental data, we consider the following function to achieve a better accuracy:

$$U(r, x) = u - U_s(A\eta^2 + 1)\exp(B\eta^2) \quad (39)$$

Note that the wind speed profile suggested in Eq. 39 is a function of radius as well as the axial distance from wind turbine. Dependency of this equation on  $x$  can be understood more clearly by examination of Eq. 34. Just behind wind turbine and in radial distance of zero from blade root, the wind speed deficit can be determined using a third rate shape, as explained in section 3.1.

Numerical wind speed profile just behind wind turbine can be calculated using BEM theory and the third rate profile mentioned above; so we can calculate the rate of mass flow passing over the wind turbine:

$$\dot{m}_{NUM} = \int \rho V \cdot dA = \int_0^{r_0} \rho V(2\pi r) dr \quad (40)$$

where

$$V = v_{nacelle}(r) + v_0 \quad (41)$$

in which  $v_{nacelle}$  is determined by means of the third rate function (Eq.8) and  $v_0$  is achieved from BEM method:

$$v_0 = (1 - a_{loc})u \quad (42)$$

Also, the mass rate of flow can be obtained by means of the analytic solution:

$$\begin{aligned} \dot{m}_{analytic} &= \int \rho U(r, x) \cdot dA \\ &= \int_0^{r_0} \rho U(r, x) 2\pi r dr \end{aligned} \quad (43)$$

where  $U(r, x)$  is the analytic wind speed profile proposed in Eq.39; thus:

$$\int_0^{r_0} \rho V(2\pi r dr) = \int_0^{r_0} \rho U(r, x) 2\pi r dr \quad (44)$$

To find the value of unknowns  $A$  and  $B$ , two equations are needed. Eq.42 provides one of these equations. Another equation is achievable using boundary condition, which implies equality of wind speed in end point of wake radius with the undisturbed wind speed:

$$x = 0 \rightarrow r_1 = r_0 \text{ and } U(r_0, 0) = u \quad (45)$$

As mentioned before,  $U_s$  is determined using Eq. 37. Note that in order for the region just behind wind turbine to use this equation,  $U_c$  must be found through the parabolic function.

Solving the above set of equations reveals the unknowns  $A$  and  $B$  and results in the analytic wind speed profile just behind wind turbine.

### 5. Calculation of Wind Speed Profile in Different Distances Downstream of Wind Turbine

Equation 39 gives a general shape of wind speed profile, which is applicable for different distances. In order to calculate the wind speed deficit in wake center and wake radius behind wind turbine, Eqs.32 and 34 are taken into account. Resolving continuity equation for control volume between distance of zero and any arbitrary distance along wind turbine axis, as shown in Fig.9, supplies one of the two equations to find unknown variables *A* and *B*.

$$\dot{m}_{NUM} + \rho\pi(r_1^2 - r_0^2)u = \int_0^{r_1} \rho U(r,x) 2\pi r dr \quad (46)$$

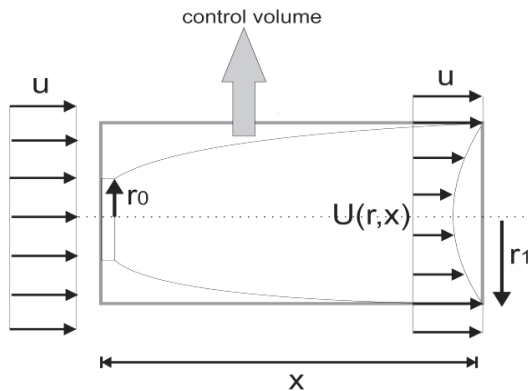


Fig.9. Control volume considered for continuity equation

Another equation can be determined again by pointing out the equality of the wind speed in end point of wake radius behind wind turbine with the undisturbed wind speed:

$$r = r_1 \rightarrow U(r_1, x) = u \quad (47)$$

Solving the above set of equations, unknown variables *A* and *B* are derived, thus the analytic wind speed profile for different distances behind wind turbine can be determined.

### 6. Results

In this research, axial and rotational induction factors using BEM theory for a wind turbine with blade specification according to Table 1 is calculated in the case when wind speed and, rotor rotational speed are 8 m/s and 30 rpm respectively, which enables one to obtain wind speed profile in distance of zero behind wind turbine. After, through the method described in section 4, analytic speed profile in this distance is calculated.

Figure 10 demonstrates speed profiles using analytic solution and BEM method just behind wind turbine. Dashed line represents BEM speed profile while solid line belongs to analytic results. As observed from the figure, the wind speed profile declines behind wind turbine and this declination depends on the wind turbine blade profile, infinity wind speed, rotational speed, and other fluid properties. The approach of this paper has the advantage to find the downstream speed profile of each point based on its radial distance as well as its axial coordinate. It can be observed from this figure that the analytic wind speed obtained from Eq.39 is in an appropriate agreement with the numerical speed profile. Another advantage of analytic speed profile in comparison to numerical one

Table 1. Blade specification [16]

r(m)	Twist (deg)	Chord (m)
4.5	20	1.63
5.5	16.3	1.597
6.5	13	1.54
7.5	10.05	1.481
8.5	7.45	1.42
9.5	5.85	1.356
10.5	4.58	1.294
11.5	4	1.229
12.5	3.15	1.163
13.5	2.6	1.095
14.5	2.02	1.026
15.5	1.36	0.955
16.5	0.77	0.881
17.5	0.33	0.806
18.5	0.14	0.705
19.5	0.05	0.545
20.5	0.02	0.265

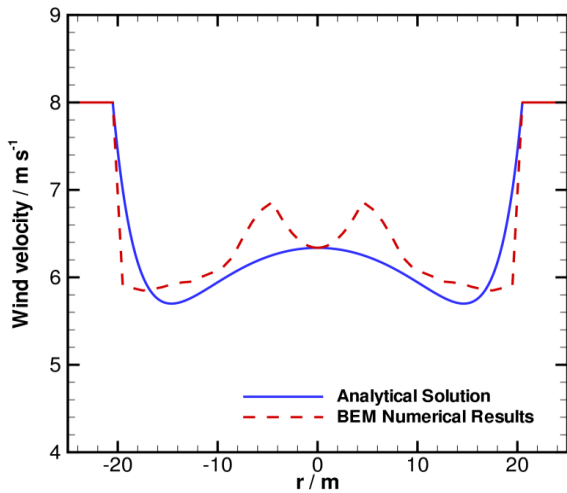


Fig.10. Comparison of analytic speed profile with speed profile obtained using BEM method in distance of zero behind wind turbine

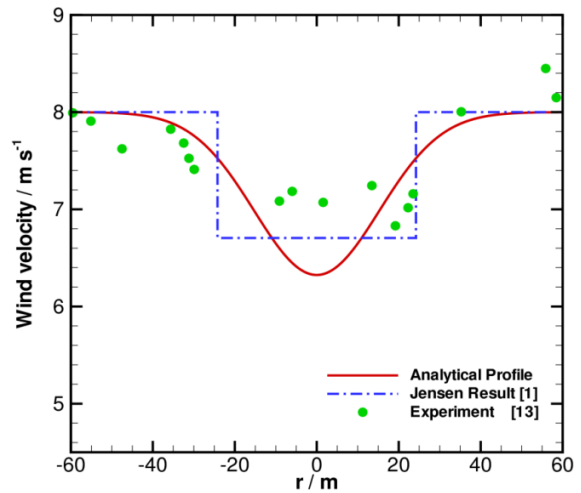


Fig.12. Comparison of analytic speed profile with experimental data from Høistруп in distance of 10 times as longer as rotor radius

appears for modeling wind speed even far from wind turbine, which is not possible numerically. In fact, calculation of wind speed profile just behind wind turbine leads to calculate the mass flow rate and therefore the wind speed profile at different downstream distances.

Approach of this study proposes wind speed profile in a region far from wind turbine, which is very interesting for site assessment purposes, according to conditions of near region behind wind turbine, which reflect the characteristics and nature of this generator of turbulence very well. For this end, it can be noticed that speed profile for this region still follows Eq.39, and the speed deficit and wake radius downstream of rotor follow Eqs.34 and 32, respectively. Figures 11 to 13 validate the analytic wind profile against experimental data from Høistруп [13].

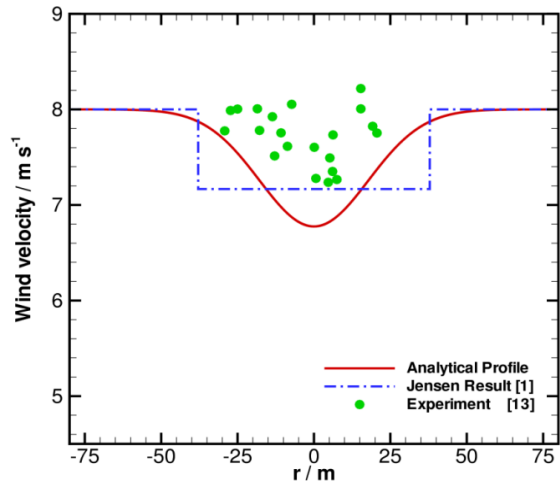


Fig.13. Comparison of analytic speed profile with experimental data from Høistруп in distance of 16 times as longer as rotor radius

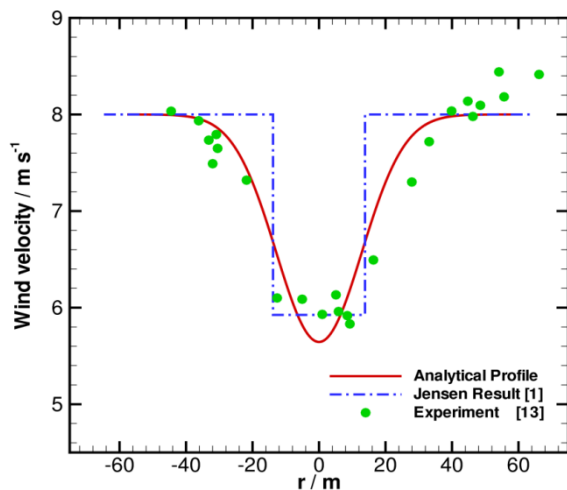


Fig.11. Comparison of analytic speed profile with experimental data from Høistруп in distance of 6 times as longer as rotor radius

In addition, these figures show speed profile calculated by means of Jensen approach for comparison. The experimental data from various fields leads to a bell-shape profile. It is evidently clear from results comparison that the method suggested here can estimate wind speed profile more realistically compared to Jensen.

### 7. Conclusion

Wind turbines produce vortex in wind flow, which crosses their rotating blades that cause wind speed deficit for their downstream wind turbines. Calculation of wind speed profile behind wind turbines is of a great interest as it enables us to estimate their wake effect on the downstream wind turbines, to optimize wind farm layout and consequently maximize the power extracted from wind flow. Wind speed

has different profiles in different points of a wind farm and must be predicted using various equations. The region behind wind turbine can be divided into two regions, close region and far region. Most of the previous researches are not able to capture wind speed profile just behind wind turbine. For the sake of wind speed profile calculation just behind wind turbine by considering its rotor blades geometrical parameters, BEM method can be exploited and a third rate function is considered to estimate speed profile behind blades hub. Wind speed profile just behind wind turbine can be obtained through calculation of mass flow rate crosses rotor area. A general shape of speed profile, which is an exponential function multiplied with a parabolic polynomial with two unknown variables (Eq. 39) is proposed to achieve a better match between experimental data and the resulted analytic speed profile. Afterward, using continuity between resulted speed profile in distance of zero and an arbitrary distance, and also, boundary condition in end point of wake radius behind wind turbine where velocity is undisturbed, both unknowns are calculated. Finally and evidently, the results are observed to match the Højstrup experimental data very well.

## References

- [1] Jensen N. O., A Note on Wind Generator Interaction, Risø National Laboratory, (1983).
- [2] Katic I., Højstrup J., Jensen N. O., A Simple Model for Cluster Efficiency, EXEC' 86 Rome, Italy, (1986).
- [3] Mosetti G., Poloni C., Diviacco B., Optimization of Wind Turbine Positioning in Large Wind Farms by Means of a Genetic Algorithm, Journal of Wind Engineering and Industrial Aerodynamics, 51, (1994) 105 - 116.
- [4] Grady S.A., Hussaini M.Y., Abdullah M.M., Placement of Wind Turbines Using Genetic Algorithms, Renewable Energy, 30, (2005) 259 - 270.
- [5] Kusiak A., Song Z., Design of Wind Farm Layout for Maximum Wind Energy Capture, Renewable Energy, 35, (2010) 685 - 694.
- [6] Chowdhury S., Zhang J., Messac A., Castillo L., Unrestricted Wind Farm Layout Optimization (UWFLO): Investigating Key Factors Influencing the Maximum Power Generation, Renewable Energy, 38, (2012) 16 - 30.
- [7] Kiranoudis C.T., Voros N.G., Maroulis Z.B., Short-cut Design of Wind Farms," Energy Policy, 29, (2001) 567 - 578.
- [8] Ozturk U. A., Norman B. A., Heuristic Methods for Wind Energy Conversion System Positioning, Electric Power Systems Research, 70, (2004) 179 - 185.
- [9] Rajper S., Amin I. J., Optimization of Wind Turbine Micrositing: A Comparative Study, Renewable and Sustainable Energy Reviews, 16, (2012) 5485 - 5492.
- [10] Gonzalez J. S., GonzalezRodraGuez A.G. Castro Mora J., Burgos Payan M., Riquelme Santos J., Overall Design Optimization of Wind Farms, Renewable Energy, 36, (2011) 1973 - 1982.
- [11] Gonzalez J. S., Gonzalez Rodriguez A. G., Castro Mora J., Riquelme Santos J., Burgos Payan M., Optimization of Wind Farm Turbines Layout Using an Evaluative Algorithm, Renewable Energy, 35, (2010) 1671 - 1681.
- [12] Frandsen S., Barthelmie R., Pryor S., Rathmann O., Larsen S., Højstrup J., Thøgersen M., Analytical Modeling of Wind Speed Deficit in Large Offshore Wind Farms, Wind Energy, 9, (2006) 39-53.
- [13] Højstrup J., Nibe Wake, Part one, Internal Technical Report, Risø, (1983).
- [14] Ghadirian A., Dehghan M., Torabi F., Considering Induction Factor Using BEM Method in Wind Farm Layout Optimization," Journal of Wind Engineering and Industrial Aerodynamics, vol. 129, (2014) 31-39.
- [15] Vermeulen P., Bultjes P., Dekker J., Van Bueren G.L., An Experimental Study of the Wake Behind a Full Scale Vertical-Axis Wind Turbine, TNO-report, (1979).
- [16] Hansen M.O.L., Aerodynamics of Wind Turbines, Taylor & Francis, (2012).
- [17] Sighard, Hoerner F., Fluid Dynamic Drag: Practical Information on Aerodynamic Drag and Hydrodynamic Resistance, Sighard, Hoerner F., (1965).
- [18] Tennekes H., Lumley J.L., A First Course in Turbulence, The MIT Press, (1972).
- [19] Prasad A.K., Analytical Solution for the Optimal Spacing of Wind Turbines," Journal of Fluids Engineering, (2014).

